MEASUREMENT OF THE INCLUSIVE $e^{\pm}p$ SCATTERING CROSS SECTION AT HIGH INELASTICITY y AND OF THE STRUCTURE FUNCTION F_L

A. PETRUKHIN

for the H1 and ZEUS Collaborations

Deutsches Elektronen-Synchrotron DESY
Notkestr. 85, 22607
Hamburg, Germany
Institute for Theoretical and Experimental Physics ITEP
Bolshaja Cheremushkinskaja 25, 117218
Moscow, Russia
E-mail: petr@mail.desy.de

Measurements are presented of the inclusive neutral current $e^{\pm}p$ scattering cross section using data collected by the H1 and ZEUS experiments at HERA during the years 2003-2007 with proton beam energies E_p of 920, 575, and 460 GeV. The measurements cover the kinematic region of absolute four-momentum transfers squared, 1.5 GeV^2 $< Q^2 <$ 120 GeV^2, small values of Bjorken x, $2.9 \cdot 10^{-5} < x < 0.01$, and extend to high inelasticity up to $y = 0.85$. The structure function F_L is measured by combining the new results with previously published data at $E_p = 920$ GeV and $E_p = 820$ GeV. The new measurements are used to test several phenomenological and QCD models applicable in this low Q^2 and low x kinematic domain.

1 Introduction

The neutral current double differential ep scattering cross section at low absolute four momentum transfer squared Q^2 in a reduced form can be represented by two structure functions:

$$\sigma_r(x, Q^2) = F_2(x, Q^2) - f(y)F_L(x, Q^2), \quad (1)$$

where $f(y) = y^2/(1+(1-y)^2)$. Here x is the Bjorken scaling variable, and the inelasticity y is related with x, Q^2 and the centre-of-mass energy squared s as $y = Q^2/(sx)$.

Due to the kinematic factor $f(y)$ and the relation $0 \leq F_L \leq F_2$, the F_L term contributes significantly to the cross section only for $y > 0.5$. In the quark-parton model, F_2 is given by the charge squared weighted sum of the quark densities while F_L is equal zero. In QCD, the gluon emission gives rise to a non-vanishing structure function F_L. Therefore, measuring F_L in the region of deep inelastic scattering (DIS) provides information about the gluon density and tests perturbative QCD as well.

2 Measurement of σ_r at high inelasticity y

One of the main aimes of the measurements presented here is to reach as high y as possible to increase the sensitivity to the structure function F_L. At low Q^2 it means to perform a measurement at low energies of the scattered electron E'_e which is difficult because of the high background of hadrons from photoproduction. Therefore, to reduce the systematic uncertainty, a special background determination procedure was developed which relies on the charge of the scattered electron candidate in data [1]. The method allows a reliable background estimation.

The cross-section measurements with different proton beam energies E_p are shown in Fig. 1. Both runs at reduced E_p extend the H1 cross section measurements at high inelasticity y (up to $y = 0.85$) down to $Q^2 = 1.5$ GeV^2. Compared to previous H1 measurements [2, 3, 4] the precision of the new data is signicantly better in the high y region. Moreover combining the H1 data at $E_p = 920$ GeV leads to an improvement in precision at high y by a factor of two.

3 Measurement of the structure function F_L

To determine the two structure functions $F_2(x, Q^2)$ and $F_L(x, Q^2)$ from the reduced cross section shown in Eq. (1) it is necessary to perform measurements at the same values of x and Q^2 but at different y. This was achieved at HERA by reducing the proton beam energy to $E_p = 460\,\text{GeV}$ and $E_p = 575\,\text{GeV}$. The run at $E_p = 460\,\text{GeV}$ gives the highest sensitivity to F_L while the run at $E_p = 575\,\text{GeV}$ extends the kinematic range of the measurement and provides a cross check. Compared to the previous H1 publication on F_L [5] we apply an improved F_L determination procedure which takes into account correlations due to systematic uncertainties. The measured structure functions F_2 and

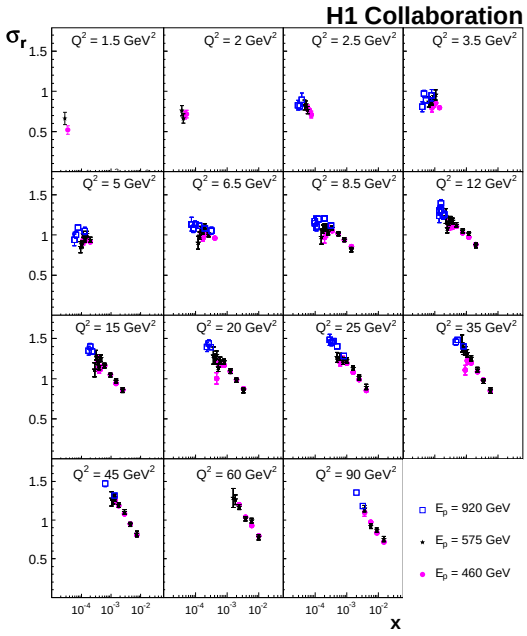

Figure 1: Results on the reduced cross section σ_r from the $E_p = 920$, 575 and 460 GeV samples. The error bars represent statistical and systematic uncertainties added in quadrature.

F_L are shown in Fig. 2 and compared to a recent result from the ZEUS [6] Collaboration. The measurement spans over two decades in x at low $0.00002 < x < 0.002$ and it is well described by a NLO DGLAP fit in the ACOT scheme [7]. We also observe a good agreement between the H1 and ZEUS data in the regions of overlap.

The values of $F_L(x; Q^2)$ resulting from averages over x at fixed Q^2 are shown in Fig. 3. The average is performed taking into account correlations. The measured structure function F_L is compared with theoretical predictions based on HERAPDF1.0 [8], CT10 [9], NNPDF2.1 [10,11], MSTW08 [12], GJR08 [13,14] and ABKM09 [15] sets. Depending on the PDF set, the calculations are performed at NLO or NNLO in perturbative QCD.

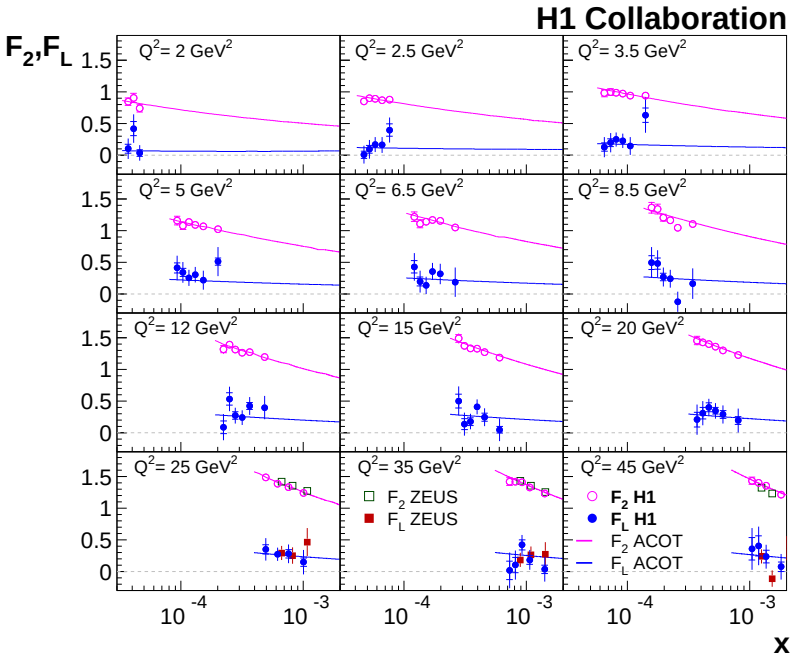

Figure 2: The proton structure functions $F_2(x;Q^2)$ and $F_L(x;Q^2)$ measured by the H1 [1] and ZEUS [6] Collaborations. The inner error bars represent the statistical error, the full error bars include the statistical and systematic uncertainties added in quadrature. The curves represent predictions of the NLO DGLAP fit in the ACOT scheme [7].

Within the uncertainties all predictions describe the data reasonably well. At low x and Q^2, where F_L is measured for the first time, some difference between the predictions is observed. The measurement of the structure functions F_2 and F_L can be used to determine the ratio $R = F_L/(F_2 - F_L)$. This ratio is shown in Fig. 4. Also results from other experiments are shown [6, 16-19]. Within the range of this measurement the ratio R is consistent with a constant behaviour with $R = 0.26 \pm 0.05$.

4 Phenomenological analysis

The combined cross-section data for E_p = 460, 575, 820 and 920 GeV are used for several phenomenological analyses. We have tested two QCD fits with different schemes for the treatment of heavy quarks and for the F_L structure function - ACOT [7] and

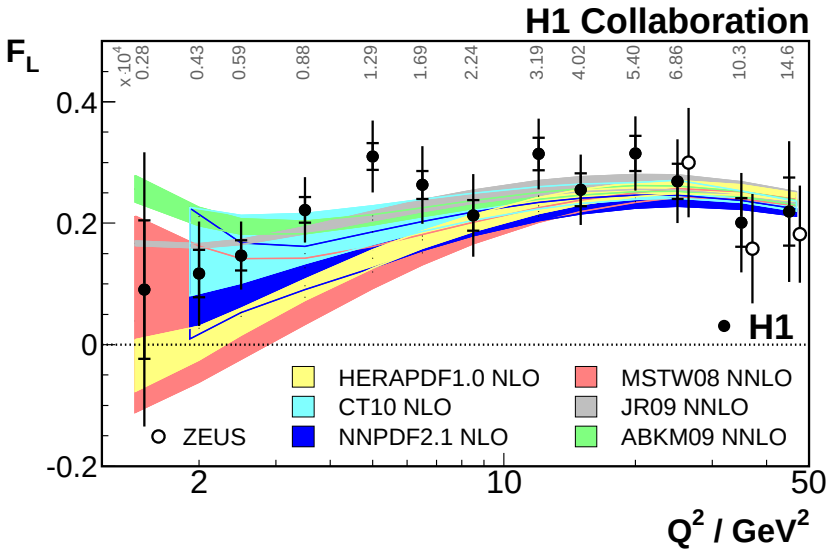

Figure 3: The proton structure function F_L shown as a function of Q^2. The average x values for each Q^2 are indicated. The inner error bars represent the statistical error, the full error bars include the statistical and systematic uncertainties added in quadrature. The bands represent predictions based on HERAPDF1.0, CTEQ6.6 and NNPDF2.1 NLO as well as MSTW08, JR09 and ABKM09 NNLO calculations.

RT [20],[21]. The ACOT fit is found to agree better with the data, having a χ^2/dof = 715/781 compared to the RT fit with χ^2/dof = 765/781. Increasing the cut on the minimum Q^2_{min} of the data used in the fit from 1.5 to 7.5 GeV^2 improves the quality of the fits. Such a change in Q^2_{min} leads to an increase of the gluon distribution while the sea-quark distribution becomes smaller at low x, see Fig. 5.

The rise of the structure function F_2 towards low x has previously been described by a power law in x, $F_2 = c(Q^2)x^{-\lambda(Q^2)}$ [22]. This simple parameterisation has been shown to model the ep data well for $x < 0.01$. This idea is extended to fit the reduced cross section σ_r in different Q^2 bins in order to simultaneously extract $\lambda(Q^2)$ and $c(Q^2)$. The parameter λ exhibits an approximately linear increase as a function of $\ln Q^2$ for $Q^2 \geq 2$ GeV^2. For lower Q^2, the variation of λ deviates from that linear dependence. The normalisation coefficient $c(Q^2)$ rises with increasing Q^2 for $Q^2 < 2$ GeV^2 and is consistent with a constant behaviour for higher Q^2, as in [22]. The quality of the fit is poor with

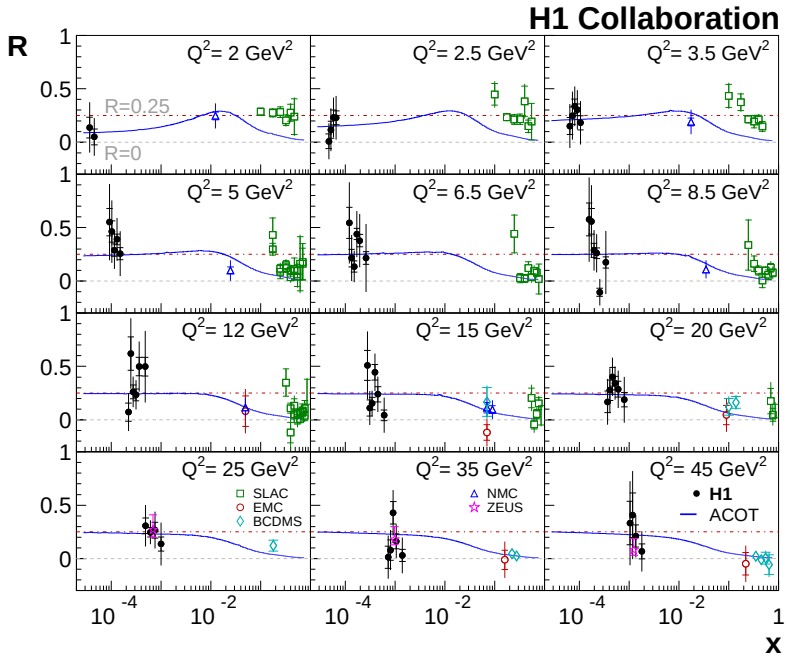

Figure 4: The ratio R as a function of x in bins of Q^2. The inner error bars represent the statistical error, the full error bars include the statistical and systematic uncertainties added in quadrature. The solid curves represent predictions of the DGLAP fit in the ACOT scheme.

the offset method for systematic error estimation: $\chi^2/dof = 538/350$. Therefore the parameterisation of F_2 was extended by one parameter to allow for deviations from a simple power law: $F_2 = c(Q^2)x^{-\lambda(Q^2)+\lambda'(Q^2)\ln x}$. This fit returns a signicantly improved $\chi^2/dof = 405/326$. Taking into account the strong correlation between λ and λ' and also the fact that λ is consistent with a constant value of $\lambda = 0.25$, we performed a fit where λ is fixed to a value of 0.25 and two parameters are free: $\lambda'(Q^2)$ and $c(Q^2)$. The quality of this fit with a total $\chi^2/dof = 464/350$ is better compared to the original λ fit. The results are shown in Fig. 6.

At low x and low Q^2, virtual photon-proton scattering can be described using the colour dipole model (CDM) [23]. In this model the initial photon splits into quark-antiquark pair (dipole) which interacts with the proton. The dipole approach is ap-

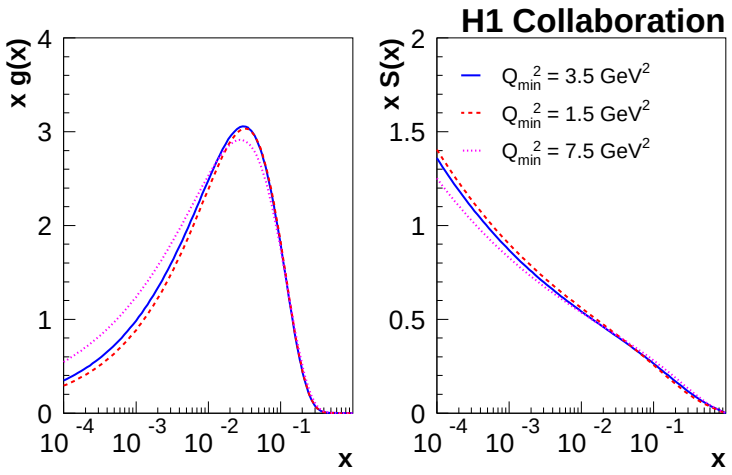

Figure 5: Gluon and sea quark PDFs shown for different values of Q^2_{min} cut.

plicable only for $x < 0.01$ where the gluon and the sea dominate since it neglects the valence contributions to the ep cross section. Hovewer these contributions can be sizable (up to 15%) also at low x. Therefore we tested three different dipole models (GBW [24], IIM [25] and B-SAT [26]) with and without a DGLAP based correction for the valence quark contributions. The fits were done in the range $3.5 \leq Q^2 \leq 150$ GeV^2 and $x < 0.01$ where both CDM and DGLAP are expected to work. It was found that the addition of the valence contribution improves the description of the data at high x, but overall fit quality is not improving.

From the models considered here the best description of the data is observed for the ACOT fit ($\chi^2/dof = 248.3/249$) which is closely followed by the pure dipole IIM fit ($\chi^2/dof = 259.4/252$). A comparison of the F_L predictions from different models to the H1 data is illustrated in Fig. 7. The data are reasonably well described by all models, except the low Q^2 region where the RT fit falls below data.

References

[1] F. D. Aaron *et al.*, Eur. Phys. J. **C71**, 1579 (2011).

[2] F. D. Aaron *et al.*, Eur. Phys. J. **C63**, 625-678 (2009).

[3] F. D. Aaron *et al.*, Eur. Phys. J. **C64**, 561-587 (2009).

[4] C. Adloff *et al.*, Eur. Phys. J. **C21**, 33-61 (2001).

[5] F. D. Aaron *et al.*, Phys. Lett. B **661**, 139-146 (2008).

[6] S. Chekanov *et al.*, Phys. Lett. B **682**, 8-22 (2009).

[7] M. Kramer, F. I. Olness and D. E. Soper, Phys. Rev. D **62**, 096007 (2000).

[8] F. D. Aaron *et al.*, JHEP **1001**, 109 (2010).

[9] H.-L. Lai *et al.*, Phys. Rev. D **82**, 074024 (2010).

[10] R. D. Ball *et al.*, Nucl. Phys. B **838**, 136 (2010).

[11] S. Forte, E. Laenen, P. Nason and J. Rojo, Nucl. Phys. B **834**, 116 (2010).

[12] A. D. Martin, W. J. Stirling, R. S. Thorne, G. Watt, [arXiv:0901.0002]

[13] M. Glueck, P. Jiminez-Delgado and E. Reya, Eur. Phys. J **C53**, 355 (2008).

[14] P. Jiminez-Delgado and E. Reya, Eur. Phys. Rev. D **79**, 074023 (2009).

[15] S. Alekhin, J. Blumlein, S. Klein and S. Moch, Phys. Rev. D **81**, 014032 (2010).

[16] J. J. Aubert *et al.*, Phys. Lett. B **121**, 87 (1983).

[17] A. C. Benvenuti *et al.*, Phys. Lett. B **223**, 485 (1989).

[18] L. W. Whitlow *et al.*, Phys. Lett. B **250**, 193 (1990).

[19] M. Arneodo *et al.*, Nucl. Phys. B **483**, 3 (1997).

[20] R. S. Thorne and R. G. Roberts, Phys. Rev. D **57**, 6871 (1998).

[21] R. S. Thorne, Phys. Rev. D **73**, 054019 (2006).

[22] C. Adloff *et al.*, Phys. Lett. B **520**, 183-190 (2001).

[23] N. N. Nikolaev and B. G. Zakharov, Z. Phys. C **49**, 607 (1991).

[24] K. Golec-Biernat and M. Wusthoff, Phys. Rev. D **59**, 014017 (1999).

[25] E. Iancu, K. Itacura and S. Munier, Phys. Lett. B **590**, 199 (2004).

[26] H. Kowalski, L. Motyka, and G .Watt, Phys. Rev. D **74**, 074016 (2006).

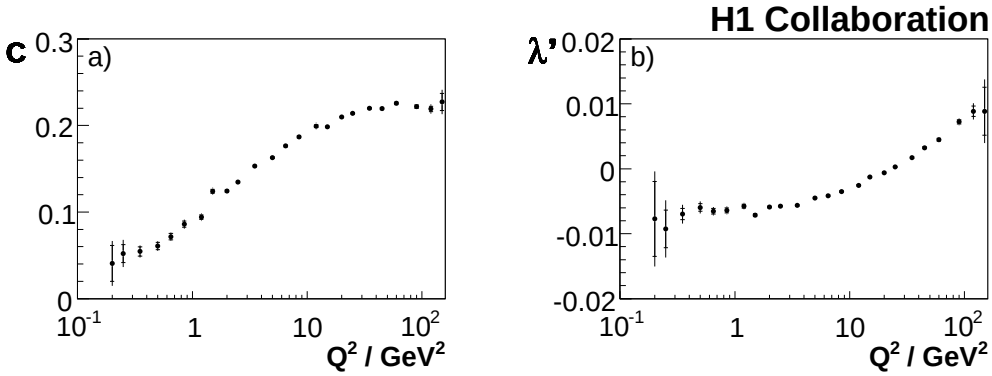

Figure 6: Coefficients c and λ' determined from a fit to the F_2 data of the form $F_2 = c(Q^2)x^{-\lambda(Q^2)+\lambda'(Q^2)\ln x}$ as a function of Q^2 with fixed $\lambda = 0.25$. The inner error bars represent the statistical uncertainties. The outer error bars contain the statistical and systematic uncertainties added in quadrature.

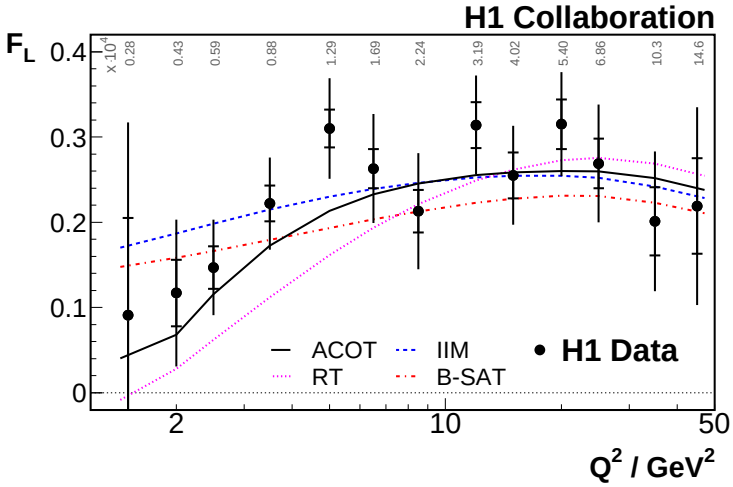

Figure 7: The proton structure function F_L and fits based on different models. The average x values for each Q^2 are indicated. The inner error bars represent the statistical error, the full error bars include the statistical and systematic uncertainties added in quadrature.